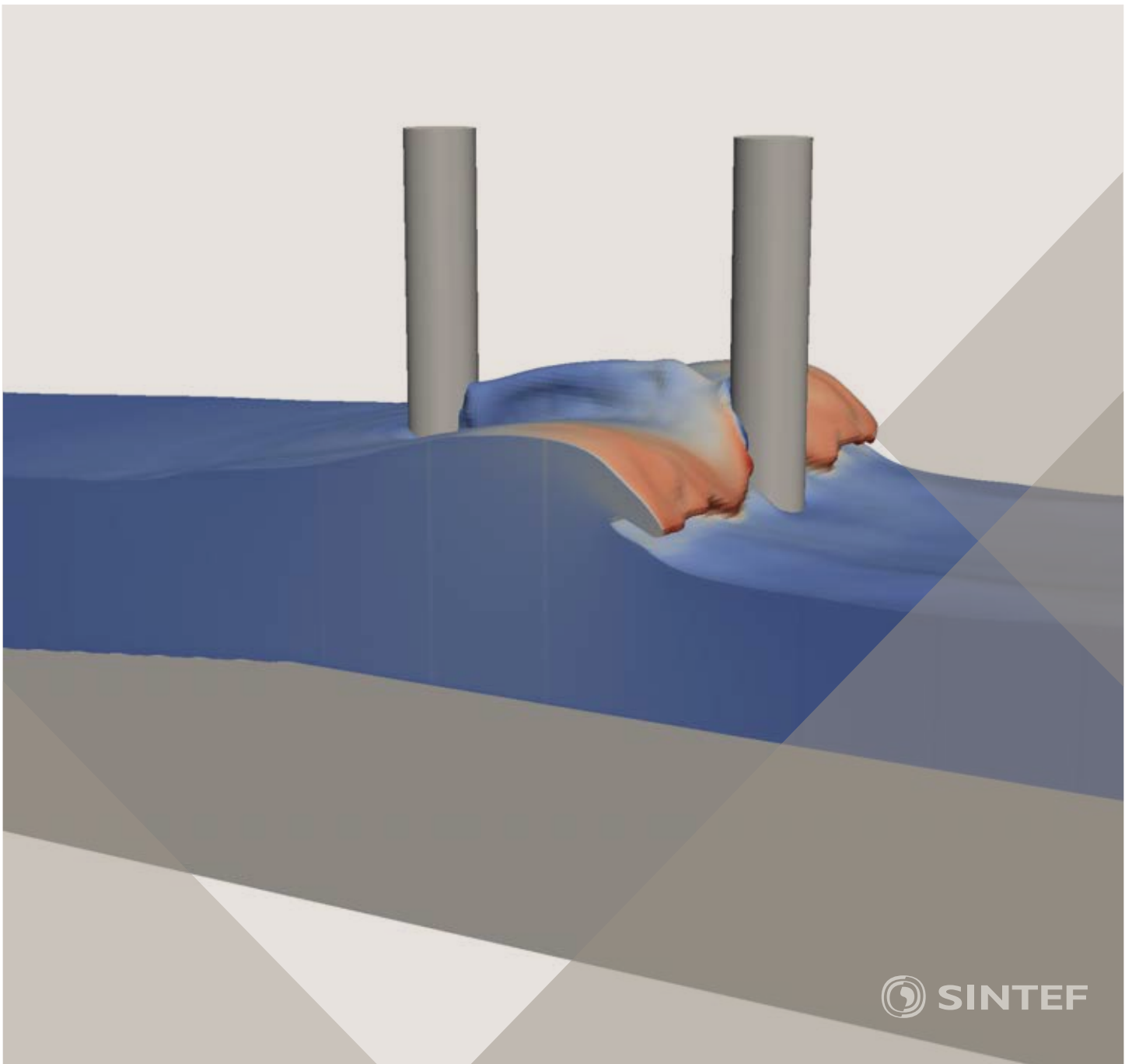


Proceedings of the 12<sup>th</sup> International Conference on  
Computational Fluid Dynamics in the Oil & Gas,  
Metallurgical and Process Industries

# Progress in Applied CFD – CFD2017



SINTEF Proceedings

Editors:

Jan Erik Olsen and Stein Tore Johansen

## **Progress in Applied CFD – CFD2017**

Proceedings of the 12<sup>th</sup> International Conference on Computational Fluid Dynamics  
in the Oil & Gas, Metallurgical and Process Industries

SINTEF Academic Press

SINTEF Proceedings no 2

Editors: Jan Erik Olsen and Stein Tore Johansen

**Progress in Applied CFD – CFD2017**

Selected papers from 10<sup>th</sup> International Conference on Computational Fluid Dynamics in the Oil & Gas, Metallurgical and Process Industries

Key words:

CFD, Flow, Modelling

Cover, illustration: Arun Kamath

ISSN 2387-4295 (online)

ISBN 978-82-536-1544-8 (pdf)

© Copyright SINTEF Academic Press 2017

The material in this publication is covered by the provisions of the Norwegian Copyright Act. Without any special agreement with SINTEF Academic Press, any copying and making available of the material is only allowed to the extent that this is permitted by law or allowed through an agreement with Kopinor, the Reproduction Rights Organisation for Norway. Any use contrary to legislation or an agreement may lead to a liability for damages and confiscation, and may be punished by fines or imprisonment

SINTEF Academic Press

Address:       Forskningsveien 3 B  
                  PO Box 124 Blindern  
                  N-0314 OSLO

Tel:             +47 73 59 30 00

Fax:            +47 22 96 55 08

[www.sintef.no/byggforsk](http://www.sintef.no/byggforsk)

[www.sintefbok.no](http://www.sintefbok.no)

**SINTEF Proceedings**

SINTEF Proceedings is a serial publication for peer-reviewed conference proceedings on a variety of scientific topics.

The processes of peer-reviewing of papers published in SINTEF Proceedings are administered by the conference organizers and proceedings editors. Detailed procedures will vary according to custom and practice in each scientific community.

## PREFACE

This book contains all manuscripts approved by the reviewers and the organizing committee of the 12th International Conference on Computational Fluid Dynamics in the Oil & Gas, Metallurgical and Process Industries. The conference was hosted by SINTEF in Trondheim in May/June 2017 and is also known as CFD2017 for short. The conference series was initiated by CSIRO and Phil Schwarz in 1997. So far the conference has been alternating between CSIRO in Melbourne and SINTEF in Trondheim. The conferences focuses on the application of CFD in the oil and gas industries, metal production, mineral processing, power generation, chemicals and other process industries. In addition pragmatic modelling concepts and bio-mechanical applications have become an important part of the conference. The papers in this book demonstrate the current progress in applied CFD.

The conference papers undergo a review process involving two experts. Only papers accepted by the reviewers are included in the proceedings. 108 contributions were presented at the conference together with six keynote presentations. A majority of these contributions are presented by their manuscript in this collection (a few were granted to present without an accompanying manuscript).

The organizing committee would like to thank everyone who has helped with review of manuscripts, all those who helped to promote the conference and all authors who have submitted scientific contributions. We are also grateful for the support from the conference sponsors: ANSYS, SFI Metal Production and NanoSim.

Stein Tore Johansen & Jan Erik Olsen



Organizing committee:

Conference chairman: Prof. Stein Tore Johansen

Conference coordinator: Dr. Jan Erik Olsen

Dr. Bernhard Müller

Dr. Sigrid Karstad Dahl

Dr. Shahriar Amini

Dr. Ernst Meese

Dr. Josip Zoric

Dr. Jannike Solsvik

Dr. Peter Witt

Scientific committee:

Stein Tore Johansen, SINTEF/NTNU

Bernhard Müller, NTNU

Phil Schwarz, CSIRO

Akio Tomiyama, Kobe University

Hans Kuipers, Eindhoven University of Technology

Jinghai Li, Chinese Academy of Science

Markus Braun, Ansys

Simon Lo, CD-adapco

Patrick Segers, Universiteit Gent

Jiyuan Tu, RMIT

Jos Derksen, University of Aberdeen

Dmitry Eskin, Schlumberger-Doll Research

Pär Jönsson, KTH

Stefan Pirker, Johannes Kepler University

Josip Zoric, SINTEF

## CONTENTS

|   |            |
|---|------------|
| <b>PRAGMATIC MODELLING .....</b>  | <b>9</b>   |
| On pragmatism in industrial modeling. Part III: Application to operational drilling .....                                       | 11         |
| CFD modeling of dynamic emulsion stability .....  | 23         |
| Modelling of interaction between turbines and terrain wakes using pragmatic approach .....                                      | 29         |
| <b>FLUIDIZED BED .....</b>  | <b>37</b>  |
| Simulation of chemical looping combustion process in a double looping fluidized bed reactor with cu-based oxygen carriers.....  | 39         |
| Extremely fast simulations of heat transfer in fluidized beds.....  | 47         |
| Mass transfer phenomena in fluidized beds with horizontally immersed membranes .....  | 53         |
| A Two-Fluid model study of hydrogen production via water gas shift in fluidized bed membrane reactors .....                     | 63         |
| Effect of lift force on dense gas-fluidized beds of non-spherical particles .....   | 71         |
| Experimental and numerical investigation of a bubbling dense gas-solid fluidized bed .....                                      | 81         |
| Direct numerical simulation of the effective drag in gas-liquid-solid systems .....   | 89         |
| A Lagrangian-Eulerian hybrid model for the simulation of direct reduction of iron ore in fluidized beds.....                    | 97         |
| High temperature fluidization - influence of inter-particle forces on fluidization behavior .....                               | 107        |
| Verification of filtered two fluid models for reactive gas-solid flows .....  | 115        |
| <b>BIOMECHANICS.....</b>  | <b>123</b> |
| A computational framework involving CFD and data mining tools for analyzing disease in carotid artery .....                     | 125        |
| Investigating the numerical parameter space for a stenosed patient-specific internal carotid artery model.....                  | 133        |
| Velocity profiles in a 2D model of the left ventricular outflow tract, pathological case study using PIV and CFD modeling.....  | 139        |
| Oscillatory flow and mass transport in a coronary artery.....   | 147        |
| Patient specific numerical simulation of flow in the human upper airways for assessing the effect of nasal surgery.....         | 153        |
| CFD simulations of turbulent flow in the human upper airways .....  | 163        |
| <b>OIL &amp; GAS APPLICATIONS .....</b>   | <b>169</b> |
| Estimation of flow rates and parameters in two-phase stratified and slug flow by an ensemble Kalman filter .....                | 171        |
| Direct numerical simulation of proppant transport in a narrow channel for hydraulic fracturing application .....                | 179        |
| Multiphase direct numerical simulations (DNS) of oil-water flows through homogeneous porous rocks .....                         | 185        |
| CFD erosion modelling of blind tees .....   | 191        |
| Shape factors inclusion in a one-dimensional, transient two-fluid model for stratified and slug flow simulations in pipes ..... | 201        |
| Gas-liquid two-phase flow behavior in terrain-inclined pipelines for wet natural gas transportation .....                       | 207        |

|   |                |
|---|----------------|
| <b>NUMERICS, METHODS &amp; CODE DEVELOPMENT .....</b>   | <b>213</b>     |
| Innovative computing for industrially-relevant multiphase flows .....   | 215            |
| Development of GPU parallel multiphase flow solver for turbulent slurry flows in cyclone.....   | 223            |
| Immersed boundary method for the compressible Navier–Stokes equations using<br>high order summation-by-parts difference operators ..... | 233            |
| Direct numerical simulation of coupled heat and mass transfer in fluid-solid systems .....  | 243            |
| A simulation concept for generic simulation of multi-material flow,<br>using staggered Cartesian grids.....                             | 253            |
| A cartesian cut-cell method, based on formal volume averaging of mass,<br>momentum equations.....                                       | 265            |
| SOFT: a framework for semantic interoperability of scientific software .....  | 273            |
| <br><b>POPULATION BALANCE .....</b>   | <br><b>279</b> |
| Combined multifluid-population balance method for polydisperse multiphase flows .....   | 281            |
| A multifluid-PBE model for a slurry bubble column with bubble size dependent<br>velocity, weight fractions and temperature.....         | 285            |
| CFD simulation of the droplet size distribution of liquid-liquid emulsions<br>in stirred tank reactors .....                            | 295            |
| Towards a CFD model for boiling flows: validation of QMOM predictions with<br>TOPFLOW experiments .....                                 | 301            |
| Numerical simulations of turbulent liquid-liquid dispersions with quadrature-based<br>moment methods.....                               | 309            |
| Simulation of dispersion of immiscible fluids in a turbulent couette flow .....   | 317            |
| Simulation of gas-liquid flows in separators - a Lagrangian approach.....   | 325            |
| CFD modelling to predict mass transfer in pulsed sieve plate extraction columns .....   | 335            |
| <br><b>BREAKUP &amp; COALESCENCE .....</b>  | <br><b>343</b> |
| Experimental and numerical study on single droplet breakage in turbulent flow .....   | 345            |
| Improved collision modelling for liquid metal droplets in a copper slag cleaning process .....  | 355            |
| Modelling of bubble dynamics in slag during its hot stage engineering.....  | 365            |
| Controlled coalescence with local front reconstruction method .....   | 373            |
| <br><b>BUBBLY FLOWS .....</b>   | <br><b>381</b> |
| Modelling of fluid dynamics, mass transfer and chemical reaction in bubbly flows .....  | 383            |
| Stochastic DSMC model for large scale dense bubbly flows.....   | 391            |
| On the surfacing mechanism of bubble plumes from subsea gas release.....  | 399            |
| Bubble generated turbulence in two fluid simulation of bubbly flow .....  | 405            |
| <br><b>HEAT TRANSFER .....</b>  | <br><b>413</b> |
| CFD-simulation of boiling in a heated pipe including flow pattern transitions<br>using a multi-field concept .....                      | 415            |
| The pear-shaped fate of an ice melting front .....  | 423            |
| Flow dynamics studies for flexible operation of continuous casters (flow flex cc).....  | 431            |
| An Euler-Euler model for gas-liquid flows in a coil wound heat exchanger.....   | 441            |
| <br><b>NON-NEWTONIAN FLOWS.....</b>   | <br><b>449</b> |
| Viscoelastic flow simulations in disordered porous media .....  | 451            |
| Tire rubber extrudate swell simulation and verification with experiments .....  | 459            |
| Front-tracking simulations of bubbles rising in non-Newtonian fluids.....   | 469            |
| A 2D sediment bed morphodynamics model for turbulent, non-Newtonian,<br>particle-loaded flows.....                                      | 479            |

|   |            |
|---|------------|
| <b>METALLURGICAL APPLICATIONS.....</b>  | <b>491</b> |
| Experimental modelling of metallurgical processes .....   | 493        |
| State of the art: macroscopic modelling approaches for the description of multiphysics phenomena within the electroslag remelting process ..... | 499        |
| LES-VOF simulation of turbulent interfacial flow in the continuous casting mold .....   | 507        |
| CFD-DEM modelling of blast furnace tapping .....  | 515        |
| Multiphase flow modelling of furnace tapholes .....   | 521        |
| Numerical predictions of the shape and size of the raceway zone in a blast furnace.....   | 531        |
| Modelling and measurements in the aluminium industry - Where are the obstacles? .....   | 541        |
| Modelling of chemical reactions in metallurgical processes.....   | 549        |
| Using CFD analysis to optimise top submerged lance furnace geometries .....   | 555        |
| Numerical analysis of the temperature distribution in a martensic stainless steel strip during hardening.....                                   | 565        |
| Validation of a rapid slag viscosity measurement by CFD.....  | 575        |
| Solidification modeling with user defined function in ANSYS Fluent.....   | 583        |
| Cleaning of polycyclic aromatic hydrocarbons (PAH) obtained from ferroalloys plant.....   | 587        |
| Granular flow described by fictitious fluids: a suitable methodology for process simulations .....  | 593        |
| A multiscale numerical approach of the dripping slag in the coke bed zone of a pilot scale Si-Mn furnace.....                                   | 599        |
| <br>  |            |
| <b>INDUSTRIAL APPLICATIONS .....</b>  | <b>605</b> |
| Use of CFD as a design tool for a phosphoric acid plant cooling pond .....  | 607        |
| Numerical evaluation of co-firing solid recovered fuel with petroleum coke in a cement rotary kiln: Influence of fuel moisture .....            | 613        |
| Experimental and CFD investigation of fractal distributor on a novel plate and frame ion-exchanger .....  | 621        |
| <br>  |            |
| <b>COMBUSTION .....</b>   | <b>631</b> |
| CFD modeling of a commercial-size circle-draft biomass gasifier.....  | 633        |
| Numerical study of coal particle gasification up to Reynolds numbers of 1000.....   | 641        |
| Modelling combustion of pulverized coal and alternative carbon materials in the blast furnace raceway .....                                     | 647        |
| Combustion chamber scaling for energy recovery from furnace process gas: waste to value .....   | 657        |
| <br>  |            |
| <b>PACKED BED.....</b>  | <b>665</b> |
| Comparison of particle-resolved direct numerical simulation and 1D modelling of catalytic reactions in a packed bed .....                       | 667        |
| Numerical investigation of particle types influence on packed bed adsorber behaviour .....  | 675        |
| CFD based study of dense medium drum separation processes .....   | 683        |
| A multi-domain 1D particle-reactor model for packed bed reactor applications.....   | 689        |
| <br>  |            |
| <b>SPECIES TRANSPORT &amp; INTERFACES .....</b>   | <b>699</b> |
| Modelling and numerical simulation of surface active species transport - reaction in welding processes .....                                    | 701        |
| Multiscale approach to fully resolved boundary layers using adaptive grids.....   | 709        |
| Implementation, demonstration and validation of a user-defined wall function for direct precipitation fouling in Ansys Fluent.....              | 717        |

|   |                |
|---|----------------|
| <b>FREE SURFACE FLOW &amp; WAVES .....</b>  | <b>727</b>     |
| Unresolved CFD-DEM in environmental engineering: submarine slope stability and other applications.....                  | 729            |
| Influence of the upstream cylinder and wave breaking point on the breaking wave forces on the downstream cylinder ..... | 735            |
| Recent developments for the computation of the necessary submergence of pump intakes with free surfaces .....           | 743            |
| Parallel multiphase flow software for solving the Navier-Stokes equations .....   | 752            |
| <br><b>PARTICLE METHODS .....</b>   | <br><b>759</b> |
| A numerical approach to model aggregate restructuring in shear flow using DEM in Lattice-Boltzmann simulations .....    | 761            |
| Adaptive coarse-graining for large-scale DEM simulations.....   | 773            |
| Novel efficient hybrid-DEM collision integration scheme.....  | 779            |
| Implementing the kinetic theory of granular flows into the Lagrangian dense discrete phase model.....                   | 785            |
| Importance of the different fluid forces on particle dispersion in fluid phase resonance mixers .....                   | 791            |
| Large scale modelling of bubble formation and growth in a supersaturated liquid.....                                    | 798            |
| <br><b>FUNDAMENTAL FLUID DYNAMICS .....</b>   | <br><b>807</b> |
| Flow past a yawed cylinder of finite length using a fictitious domain method .....                                      | 809            |
| A numerical evaluation of the effect of the electro-magnetic force on bubble flow in aluminium smelting process.....    | 819            |
| A DNS study of droplet spreading and penetration on a porous medium.....  | 825            |
| From linear to nonlinear: Transient growth in confined magnetohydrodynamic flows.....                                   | 831            |

## SIMULATION OF GAS-LIQUID FLOWS IN SEPARATORS. A LAGRANGIAN APPROACH

John C. MORUD<sup>1\*</sup>, Sigrid K. DAHL<sup>1†</sup>

<sup>1</sup>SINTEF Materials and Chemistry, 7465 Trondheim, NORWAY

\* E-mail: john.morud@sintef.no

† E-mail: sigrid.k.dahl@sintef.no

### ABSTRACT

In order to simulate the separation efficiency of gas scrubbers, we have formulated and implemented a version of the Single-Particle Method. The method is suitable for CFD simulations of gas-droplet flows, and is based on using Lagrangian tracking of droplets. An implementation of the method has been made in a commercial CFD tool. The methodology and the CFD implementation have been validated against analytical results in the literature.

**Keywords:** CFD; fluid mechanics; two-phase; multi-phase; droplets; population balance .

|                      |   |
|----------------------|---|
| $N$                  | Number of field particles in cell, [-]                            |
| $S$                  | Source term in population balance, [ $kg/m^3 \cdot m^3 \cdot s$ ] |
| $t$                  | Time, [s]   |
| $\Delta t$           | Time step, [s]  |
| $T_L$                | Lagrangian time scale of turbulence, [s]                          |
| $\mathbf{u}$         | Velocity in pop. balance, [ $m/s$ ]                               |
| $\mathbf{u}_{fluid}$ | Velocity of continuous fluid, [ $m/s$ ]                           |
| $v$                  | Droplet volume (size), [ $m^3$ ]                                  |
| $V_{cell}$           | Volume of Finite Volume cell, [ $m^3$ ]                           |
| $\mathbf{x}$         | Position in space, [ $m$ ]  |
| $y_i$                | Volume (size) of field particle 'i', [ $m^3$ ]                    |

### NOMENCLATURE

#### Greek Symbols

|               |   |
|---------------|---|
| $\beta$       | Under-relaxation factor for mass field, [-]                   |
| $\beta(v v')$ | Mass distribution, daughter droplets in breakup, [ $m^{-3}$ ] |
| $\Gamma$      | Breakup rate, [ $s^{-1}$ ]                                    |
| $\delta$      | Typical cell dimension, [ $m$ ]                               |
| $\varepsilon$ | Turbulent dissipation rate, [ $W/kg$ ]                        |
| $\lambda$     | Replacement rate constant for field particles, [ $1/s$ ]      |
| $\xi$         | Random number or process [-]                                  |
| $\rho_{liq}$  | Liquid density, [ $kg/m^3$ ]                                  |
| $\tau$        | Residence time for droplet, [s]                               |
| $\varphi_i$   | Concentration of field particles, [ $kg/m^3$ ]                |
| $\phi$        | Particle field, [ $kg/m^3 \cdot m^3$ ]                        |
| $\chi$        | Coalescence rate, [ $s^{-1}$ ]                                |

#### Latin Symbols

|             |   |
|-------------|---|
| $d$         | Droplet diameter, [ $m$ ]                               |
| $F$         | Cumulative size distribution, [-]                       |
| $K$         | Coalescence kernel, [ $m^3/s$ ]                         |
| $k$         | Turbulent kinetic energy, [ $m^2/s^2$ ]                 |
| $k_b$       | Parameter in Case 1 and 3, [ $s^{-1}$ ]                 |
| $L_E$       | Turbulent correlation length, [ $m$ ]                   |
| $m(v)$      | Size distribution on mass basis, [ $kg/m^3 \cdot m^3$ ] |
| $\dot{m}$   | Mass flow rate of droplets, [ $kg/s$ ]                  |
| $\tilde{M}$ | Temporary field, [ $kg/cell$ ]                          |
| $M$         | Mass of droplets in cell, [ $kg/cell$ ]                 |

### INTRODUCTION

In many gas-liquid separation applications the separation efficiency is critically dependent on the particle size of the dispersed phase. Frequently, the use of an average particle size is sufficient for fluid flow simulations. However, there are a number of applications where one should consider the complete particle size distribution. The motivation for the work in this paper stems from high pressure gas-liquid separation (scrubbers) where there is a small amount of low surface tension liquid in a gas flow. However, most of the methodology is directly applicable to general multiphase flows as well as population balances occurring in Chemical Engineering applications, such as crystallizers.

The most important phenomena in scrubber applications are *droplet coalescence*, *droplet breakup*, *droplet deposition on walls* and *entrainment of droplets from walls*. The methodology in this paper is applicable to these, allowing a user to predict the performance of coalescence and breakup kernels and compare the predictions to experimental data. Actual physical models and validation against high pressure data will be a topic for a subsequent paper. Thus, in this paper we consider a droplet population balance with coalescence and breakup and show how it can be solved for arbitrary kernels.

There are a number of possible strategies for population balance simulations. One approach is to apply a quadrature rule to the integrals occurring in the population balance and track information in an Eulerian fashion. Among such methods are the Method of Classes (Ramkrishna, 2000); Galerkin methods; the method of Least Squares (Jiang, 1998; Dorao and Jakobsen, 2005); Orthogonal Collocation techniques and moment methods (McGraw, 1997). See also Morud (2011), Attarakih *et al.* (2004) and Attarakih *et al.* (2009).

Another way is by treating the dispersed phase as Lagrangian particles and track them throughout the flow field. The Lagrangian approach is particularly simple to implement for breakup dominated flows, as long as breakup events involve only the breaking particle and not the interaction between particles. Also aggregation events can be handled by counting and computing particle statistics in the numerical mesh (Haviland and Lavin, 1962).

In this paper we present a Lagrangian method based on the Single-Particle method of Vikhansky and Kraft (2005) together with the steady state Discrete-Particle-Method (DPM) in ANSYS FLUENT v13.0.0.

The paper is organized as follows: First the concept for handling coalescence by means of field particles is explained in an Eulerian framework. Then the Lagrangian formulation is described, explaining how to handle coalescence and breakup in the steady state DPM model. The methodology is validated against analytical solutions in the literature. Finally, we demonstrate our CFD implementation using a simple test example.

## MODEL DEVELOPMENT

We use a simple Eulerian population balance as a point of departure for the formulation of our Lagrangian model. In this manner the relation between source terms in the two formulations become apparent, allowing us to translate coalescence and breakup kernels from an Eulerian model into the Lagrangian model.

For laminar flow and at steady state the two stated models are equivalent, and can be directly compared. However, our Lagrangian formulation differs from the stated Eulerian model in that it is essentially a steady state model. Moreover, Lagrangian particles have individual velocities allowing for turbulent dispersion of equal particles. The stated Eulerian formulation is simpler in this respect as particles of equal size and position have the same velocity.

### Eulerian formulation

The droplet size distribution on mass basis at a given point in time and space,  $m(v)$ , is illustrated in Figure 1. Here  $v [m^3]$  is the droplet size (volume). Thus, within an infinitesimal size range between droplet size  $v [m^3]$  and  $v + dv [m^3]$ , the mass of droplets is  $m(v) dv [kg/m^3]$ .

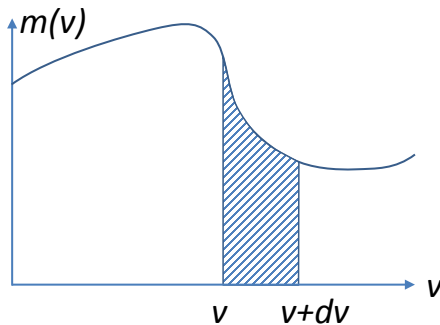


Figure 1: Droplet size distribution.

In an Eulerian framework the development of the droplet size distribution can be described by a population balance equa-

tion

$$\frac{\partial m(v, \mathbf{x}, t)}{\partial t} + \nabla \cdot (\mathbf{u}(v, \mathbf{x}, t) m(v, \mathbf{x}, t)) = S(v, \mathbf{x}, t) \quad (1)$$

where  $v$ ,  $\mathbf{x}$  and  $t$  are the droplet volume, position and time;  $\mathbf{u}(v, \mathbf{x}, t) [m/s]$  is the velocity field of the droplets and  $S(v, \mathbf{x}, t)$  is the source term consisting of birth and death of droplets due to coalescence and breakup. In the following we will omit  $\mathbf{x}$  and  $t$  for convenience as they are always present.

In particular, the birth by coalescence on mass basis is

$$S_{coal}^B(v) = \int_0^v \frac{K(v-v', v')}{\rho_{liq} v'} m(v') m(v-v') dv' \quad (2)$$

where  $K [m^3/s]$  is the coalescence kernel and  $\rho_{liq} [kg/m^3]$  is the liquid density. The integral combines all pairs of droplet sizes,  $v'$  and  $v-v'$ , that sums to droplet size  $v$ . Following Vikhansky and Kraft (2005) this can be written formally as

$$S_{coal}^B(v) = \int_0^v \frac{K(v-v', v')}{\rho_{liq} v'} \phi(v') m(v-v') dv' \quad (3)$$

where  $\phi(v)$  is equal to the mass distribution  $m(v)$  at a converged solution. We follow Vikhansky and Kraft (2005) and denote  $\phi(v)$  as the field (or target) particles. The basic principle is to keep an approximation to  $\phi(v)$  within each Finite Volume cell, whereas  $m(v)$  is represented by the Lagrangian simulation particles. An updating scheme is then introduced, which will make  $m(v)$  and  $\phi(v)$  equal at steady state.

The corresponding death term by coalescence becomes

$$S_{coal}^D(v) = - \int_0^\infty \frac{K(v, v')}{\rho_{liq} v'} \phi(v') m(v) dv' \quad (4)$$

Finally, we have the birth and death terms by breakup

$$S_{break}^B(v) = \int_v^\infty \Gamma(v') \beta_m(v|v') m(v') dv' \quad (5)$$

$$S_{break}^D(v) = -\Gamma(v) m(v) \quad (6)$$

where  $\Gamma(v) [1/s]$  is the breakage frequency and  $\beta_m(v|v')$  is the mass distribution of the daughter droplets resulting from the breakage of a droplet of size  $v'$ .

### Lagrangian formulation

The population balance, equation (1), can be written in a Lagrangian reference frame following a droplet:

$$\frac{d\mathbf{x}}{dt} = \mathbf{u} \quad (7)$$

$$\frac{d\mathbf{u}}{dt} = \mathbf{f}(v, \mathbf{u}, \mathbf{u}_{fluid}, \dots) \quad (8)$$

$$\frac{dv}{dt} = G(v) \quad (9)$$

$$\frac{dm}{dt} = S(v) - m \cdot \text{div}(\mathbf{u}) \quad (10)$$

where  $\mathbf{u}_{fluid}$  is the velocity of the continuous fluid,  $\mathbf{f}$  is the force per droplet mass and  $G$  is the growth rate of a droplet (normally zero in our models). As before,  $\mathbf{x}$  and  $t$  are omitted from the argument lists for convenience. Note that the continuous fluid is still represented in an Eulerian reference frame.

The two first equations are Newton's second law of motion for a droplet. In our case, we use the Discrete Particle Model (DPM) of FLUENT. Thus, we use the CFD code to track particles for us.

The third equation describes the growth of a droplet, which is normally zero in our models as we are considering breakup and coalescence only<sup>1</sup>.

The last equation shows that the mass density distribution along a droplet path varies due to (a) the source term,  $S$ , and (b) whether droplets approach each other or move apart. The equation is derived by applying the chain rule to  $m$  along a droplet track, i.e.

$$\frac{dm}{dt} = \frac{\partial m}{\partial t} + (\mathbf{u} \cdot \nabla) m = \underbrace{\frac{\partial m}{\partial t} + \nabla \cdot (\mathbf{u}m)}_{S(v)} - m (\nabla \cdot \mathbf{u}) \quad (11)$$

The source term for a Lagrangian **material volume**,  $\Omega(v)$ , of droplets of size  $v$  is the **same** as for the Eulerian formulation, namely  $S(v)$ . To see this, consider a material volume of droplets of size  $v$ , i.e. a material control volume with a boundary that follows the droplet velocity field for this size,  $\mathbf{u}(v)$ . There is no droplet flux of size- $v$  droplets across its boundary. The rate of change of the size distribution within this volume can then be found by using the Reynolds transport theorem followed by the Gauss theorem:

$$\begin{aligned} \frac{d}{dt} \left[ \int_{\Omega(v)} m dV \right] &= \int_{\Omega(v)} \frac{\partial m}{\partial t} dV + \int_{\partial\Omega(v)} m \mathbf{u} \cdot d\mathbf{A} \\ &= \int_{\Omega(v)} \frac{\partial m}{\partial t} dV + \int_{\Omega(v)} \nabla \cdot (\mathbf{u}m) dV \\ &= \int_{\Omega(v)} \left[ \frac{\partial m}{\partial t} + \nabla \cdot (\mathbf{u}m) \right] dV \\ &= \int_{\Omega(v)} S(v) dV \end{aligned} \quad (12)$$

Thus, in this interpretation the source term is the same for both the Eulerian and the Lagrangian frames.

### Lagrangian simulation particles

In our method we use the concept of *simulation particles*, which differs slightly from that of individual droplets. The use of simulation particles is abundant in the literature.

One extreme would be to represent every droplet by a simulation particle. We denote this as an *analog simulation*. This is not commonly used due to the computational cost, as the number of droplets in realistic cases is quite high. The other extreme is to consider Lagrangian tracking as a form of discretization of a continuous transport equation. Thus, the simulation particles are considered to be *virtual*. In this sense we can make simulation particles for any transport equation, say the equation for turbulent kinetic energy or for the dissipation rate.

In the present work, a simulation particle represents a group of droplets of similar size and follows the laws of motion of a representative droplet in the group. In the steady state model the path of the simulation particle represents a mass flow rate

<sup>1</sup> For the coalescence and breakage source terms, Equations (3), (4), (6), the growth term  $G$  becomes zero. This can be seen by subtracting  $\rho_{liq}v$  times the number density population balance from the mass density population balance, and thus obtain an equation for the evolution of droplet mass,  $d(\rho_{liq}v)/dt$ , in the Lagrangian frame. The breakup source term cancels. Due to the symmetry of the coalescence kernel,  $K(x,y) = K(y,x)$ , the coalescence term also cancels. Thus, droplets appear and disappear but do not grow or shrink by coalescence and breakup.

of droplets of similar size. Thus, we associate a mass flow rate,  $\dot{m}$  [kg/s], and a droplet size,  $v$  [ $m^3$ ], with the simulation particle.

### Monte Carlo methods

We are usually only interested in the average behavior of a large number of simulation particles, which means that techniques from Monte Carlo particle methods can be used (see Lux and Koblinger (1991)). Basically, we can choose how many realizations of a stochastic process we use provided that the number of realizations is large enough.

A basic Monte Carlo method is the one provided by the standard FLUENT DPM model with turbulent dispersion. We select particles randomly at the inlet based on the inlet size distribution and track them throughout the domain. Each of these particle tracks is associated with a liquid mass flow,  $\dot{m}$ .

There are a few observations to be made that greatly simplify our Lagrangian scheme. This is discussed in the following.

### Statistical weights

The key observation is that the mass flow,  $\dot{m}$ , of a particle track can be thought of as a statistical weight in the sense of Lux and Koblinger (1991). That is, given that a track is only one of a very large number of tracks, it results in only a small perturbation of the solution and the expected impact on the computed results becomes proportional to  $\dot{m}$ . Formally, and as a theoretical device for the subsequent discussion only, let us write this as

$$\Delta R = \dot{m} \cdot r(\mathbf{z}_0, \xi) \quad (13)$$

where  $\Delta R$  is the change in the results (i.e. some value, say the calculated separation efficiency),  $r$  is the impact on  $R$  per unit mass flow,  $\mathbf{z}_0$  is a state vector describing the initial state of the particle and  $\xi$  is a stochastic process (a vector of random numbers that decides what happens to the particle during tracking).

### Monte Carlo splitting

Assume that we choose to realize a given simulation particle by *two* particle tracks instead of one. We split the mass flow,  $\dot{m}$ , of the particle between the two realizations as  $\dot{m} = \dot{m}_1 + \dot{m}_2$  and simulate them independently. We then get an impact which is the sum of the two.

$$\Delta R_* = \dot{m}_1 \cdot r(\mathbf{z}_0, \xi_1) + \dot{m}_2 \cdot r(\mathbf{z}_0, \xi_2) \quad (14)$$

Note that the stochastic processes  $\xi_1$  and  $\xi_2$  are now different as there are two different realizations. Also note that two realizations use the same droplet size as the original particle; only the associated mass flow rates differ.

The expected value of  $r$  is independent of any actual realization  $\xi$  since it is the average of all possible realizations starting at state  $\mathbf{z}_0$ .

$$E[r(\mathbf{z}_0, \xi)] = E[r(\mathbf{z}_0, \xi_1)] = E[r(\mathbf{z}_0, \xi_2)] \quad (15)$$

Thus, the expected value stays the same as before:

$$\begin{aligned} E[\Delta R_*] &= \dot{m}_1 \cdot E[r(\mathbf{z}_0, \xi_1)] + \dot{m}_2 \cdot E[r(\mathbf{z}_0, \xi_2)] \\ &= (\dot{m}_1 + \dot{m}_2) \cdot E[r(\mathbf{z}_0, \xi)] \\ &= E[\Delta R] \end{aligned} \quad (16)$$

In summary, expected values do not change if we split a simulation particle into two and use different realizations for the two.

### Monte Carlo selection

Another modification is selection between two different particle tracks with mass flows  $\dot{m}_1$  and  $\dot{m}_2$ . We consider two different simulation particles with initial states,  $\mathbf{z}_1$  and  $\mathbf{z}_2$ . The impact of the two becomes

$$\Delta R_s = \dot{m}_1 \cdot r(\mathbf{z}_1, \xi_1) + \dot{m}_2 \cdot r(\mathbf{z}_2, \xi_2) \quad (17)$$

Now, consider realizing only one of the particles. With probability  $p_1 = \frac{\dot{m}_1}{\dot{m}_1 + \dot{m}_2}$  we simulate only particle 1. Otherwise, we simulate particle 2. We use the total mass flow for the selected particle. Thus with probability  $p_1$  we get

$$\Delta R_{s1} = (\dot{m}_1 + \dot{m}_2) \cdot r(\mathbf{z}_1, \xi_1) \quad (18)$$

otherwise, with probability  $p_2 = 1 - p_1$  we get

$$\Delta R_{s2} = (\dot{m}_1 + \dot{m}_2) \cdot r(\mathbf{z}_2, \xi_2) \quad (19)$$

The overall expected value of this operation becomes

$$\begin{aligned} & E[\Delta R_{s*}] \\ &= p_1 E[\Delta R_{s1}] + p_2 E[\Delta R_{s2}] \\ &= p_1 E[(\dot{m}_1 + \dot{m}_2) \cdot r(\mathbf{z}_1, \xi_1)] + p_2 E[(\dot{m}_1 + \dot{m}_2) \cdot r(\mathbf{z}_2, \xi_2)] \\ &= p_1 (\dot{m}_1 + \dot{m}_2) E[r(\mathbf{z}_1, \xi_1)] + p_2 (\dot{m}_1 + \dot{m}_2) E[r(\mathbf{z}_2, \xi_2)] \\ &= \dot{m}_1 E[r(\mathbf{z}_1, \xi_1)] + \dot{m}_2 E[r(\mathbf{z}_2, \xi_2)] \\ &= E[\Delta R_s] \end{aligned} \quad (20)$$

Thus, the expected value stays the same as if both particles were simulated. In summary, we are at liberty to pick two simulation particles (with mass flows  $\dot{m}_1$  and  $\dot{m}_2$ ), select one of these with probabilities  $p_1 = \dot{m}_1 / (\dot{m}_1 + \dot{m}_2)$  and  $p_2 = 1 - p_1$  respectively and simulating only the selected particle using a mass flow  $\dot{m} = \dot{m}_1 + \dot{m}_2$ .

### Application of splitting to coalescence events

Using Monte Carlo splitting, a simulation particle can be split into several simulation particles at any point of the particle track as long as the total mass flow rate of droplets stays the same. In particular, this means that the resulting droplet from a binary coalescence event can be represented by *two* simulation particles, with mass flows corresponding to the droplets entering the coalescence event. This simplifies book-keeping, since a binary coalescence can then be modeled as an interaction between two particle tracks where the simulation particles preserve their mass flows but change diameters in the interaction. In the actual implementation of the single-particle method, each of these simulation particles interacts only with the field particles, simplifying the book-keeping even further.

The model development proceeds in four stages, as illustrated in Figure 2.

- (a) We start with the coalescence event. Two particles with mass flows  $\dot{m}_1$  and  $\dot{m}_2$  collides, and a daughter particle with mass flow  $\dot{m}_1 + \dot{m}_2$  is produced. The droplet size becomes  $v_1 + v_2$

- (b) We could use two realizations to simulate the daughter particle. The realizations would have mass flows  $\dot{m}_1$  and  $\dot{m}_2$ . As explained in section this modification does not change expected values of the Monte Carlo simulation. That is, we obtain the same result on average as if we use scheme (a). Note that both daughter realizations have droplet size  $v_1 + v_2$ .
- (c) This is the same as (b), but illustrates that we could reuse the simulation particles entering the collision to simulate the two realizations of the daughter particle. Thus, the book-keeping becomes simpler as we consider a coalescence as an interaction between two simulation particles. The simulation particles change droplet size to  $v_1 + v_2$  during the interaction, whereas the mass flow,  $\dot{m}$ , stays the same.
- (d) Finally, we replace one of the simulation particles with the mean field,  $\phi$ , which is a statistical representation of the particles. In the present scheme, we sample simulation particles that pass through the Finite Volume cells and pick collision events randomly from this sample.

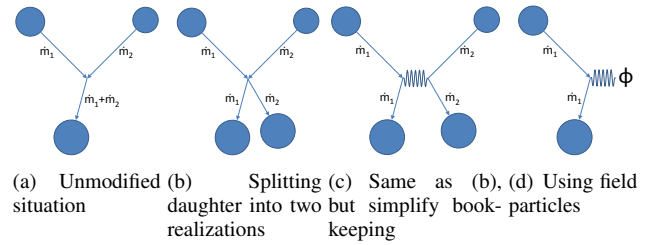


Figure 2: Development of coalescence scheme

### Application of selection to breakup events

In the same manner, we can simplify breakup events. When a droplet breaks into daughters we select one of the daughters by sampling a random droplet size,  $v$ , from the daughter distribution,  $\beta_m(v|v')$ . The mass flow of the simulation particle is thus kept during breakup events, whereas the diameter becomes that of the selected daughter. Expected values are preserved in this operation, meaning that the average behavior of a large number of tracks is the same as if every daughter were tracked. As before, we re-use the simulation particle entering the breakup event to simulate the selected daughter particle.

The situation is illustrated in Figure 3.

- (a) We start with a breakup event, illustrated by a binary breakup into droplets of size  $v_1$  and  $v_2$ .
- (b) Using Monte Carlo selection we realize only one of the daughters. We select a random droplet size by sampling the daughter distribution,  $\beta_m(v|v')$ , and using the total mass flow  $\dot{m}$ . This method is a continuous extension of the selection procedure explained in the section "Monte Carlo selection" above; thus this modification does not change expected values in the simulation.

### The FLUENT DPM model

To simulate particle tracks following Newton's second law of motion we use the Discrete Particle Model (DPM) of Ansys FLUENT. For turbulent flow, we use their standard

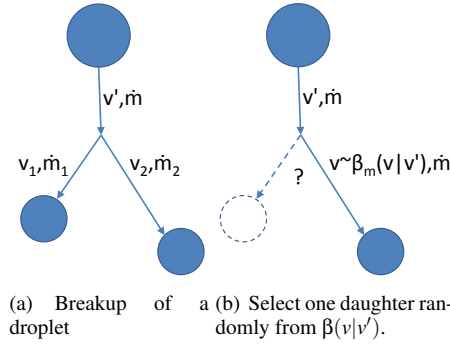


**Figure 3:** Development of breakup scheme

$k - \epsilon$  model together with the Discrete Random Walk (DRW) model. The DRW model simulates the interaction of a particle with a succession of discrete stylized turbulent eddies (Ansys Inc., Nov. 2010). Fluid velocity fluctuations are sampled from a Gaussian probability distribution assuming isotropic turbulence and a turbulent kinetic energy  $k$  provided by the  $k - \epsilon$  model. The interaction lasts for a duration that is the minimum of the Lagrangian time scale,  $T_L = C_L k / \epsilon$ , of the fluid and an eddy crossing time explained in the cited reference.

Thus, we write our population balance model on top of the existing DPM model in FLUENT by handling the population balances at the end of each time step of the DPM model. In this manner, our formulation inherits all the functionality of the DPM model. All we do is to add population balance functionality to the existing model.

### Lagrangian formulation for simulation particles

Thus, to simulate particle tracks we perform the following:

1. At the fluid inlet, pick simulation particles randomly from the inlet size distribution. The inverse distribution method is suitable, i.e. generate droplet volumes according to  $v = F^{-1}(\xi)$  where  $\xi$  is a uniform on  $[0,1]$  random number and  $F(v)$  is the cumulative size distribution, i.e. the fraction of the droplet mass below size  $v$ .
2. Simulate particle tracks according to Newton's second law of motion, and handle coalescence, breakup and deposition events at each time step. The actual tracking of the particle is handled by FLUENT's DPM model. All we do is to handle breakup and coalescence.

The details of the particle tracking are given in the following sections.

### Tracking particles

At each time step, perform the following tasks:

1. Update the overall mass holdup of droplets in the current FV-cell.
2. Update the field particles in the current cell.
3. Handle coalescence.
4. Handle breakup.

Each of these is described subsequently.

### Updating the overall mass holdup of droplets

As each particle track represents a mass flow rate,  $\dot{m}$ , of droplets, the mass holdup represented by one time step,  $\Delta t$ , of a simulation particle becomes  $\dot{m}\Delta t$ . Define a mass field of droplets,  $M$  [kg/cell], and a temporary field  $\tilde{M}$  [kg/cell].

Before each particle track: Set  $\tilde{M} = 0$ .

At each particle time step during a track: Add the holdup contribution  $\dot{m}\Delta t$  to the temporary field  $\tilde{M}$  of the current Finite Volume cell. If the cell differs from the previous cell, split the holdup contribution equally between the new and the previous cell (Nothing is gained by interpolating individual tracks linearly as the expected value of the split ratio is 50-50, which means that an equal split is correct on average for a large number of tracks).

At the end of a particle track: Update the mass field of droplets as  $M := \beta\tilde{M} + (1 - \beta)M$  where  $\beta$  is an under-relaxation factor. A typical value of  $\beta$  in our simulations is of the order of  $\beta \approx 0.01$ , which means that the mass field  $M$  is an exponential average of roughly the previous 100 particle tracks.

### Updating the field particles of the current cell

Updating the field particles in a Finite Volume (FV) cell is based on keeping statistics of the simulation particles that have visited the cell so far. This can be done in several ways, e.g. by means of histograms (Haviland and Lavin, 1962). Here, we follow Vikhansky and Kraft (2005) and represent the field particle ensemble in a FV cell by  $N$  particle groups with sizes  $y = [y_1, y_2, \dots, y_i, \dots, y_N]$ . A simple updating scheme is to pick a random number  $n$  using a Poisson distribution with parameter  $\lambda\Delta t$  where  $\Delta t$  is the time step and  $\lambda$  is a constant parameter. Replace  $n$  of the field particles in the current cell by the simulation particle. Store the size and the velocity of field particles.

Note that the number  $N$  of field particles in a FV cell is fixed. Moreover, this number can be small if the FV cells are small as long as the number of field particles per fluid volume is sufficient.

We choose the number of field particles per cell,  $N$ , to have a sufficient density of field particles. I.e.  $N/\delta^3$  should be sufficiently large, where  $\delta$  [m] is a typical cell dimension. The appropriate value of  $N$  should be selected from a sensitivity test.

We choose the parameter  $\lambda$  in the field particle replacement by setting the ratio  $\lambda\tau/N$  to a small value, say 0.01, where  $\tau$  is a typical residence time for a simulation particle in a cell. The ratio represents the fraction of the field particles in a cell that is replaced by a simulation particle on average.

### Handling coalescence

In the current scheme, simulation particles collide with field particles. There are  $N$  field particles in a FV cell with a total mass  $M$ , i.e. the mass of each field particle in a cell is  $M/N$ .

The field particles can be thought of as a discrete particle density distribution

$$\phi(v) = \sum_i \varphi_i \delta(v - y_i) = \sum_i \left( \frac{M}{NV_{cell}} \right) \delta(v - y_i) \quad (21)$$

where  $\phi_i = \frac{M}{NV_{cell}}$  is the mass concentration of field particle  $i$  in the cell,  $\delta(v - y_i)$  is a Dirac delta function at droplet volumes  $y_i$  and  $V_{cell}$  [ $m^3$ ] is the cell volume.

The death term for coalescence can then be written as:

$$\begin{aligned} S_{coal}^D(v) &= - \int \frac{K(v,v')}{\rho_{liq} v'} \phi(v') m(v) dv' \\ &= - \int \frac{K(v,v')}{\rho_{liq} v'} [\sum_i \phi_i \delta(v' - y_i)] m(v) dv' \\ &= -m(v) \sum_i \phi_i \underbrace{\frac{K(v,y_i)}{\rho_{liq} y_i}}_{\chi_i(v)} \end{aligned} \quad (22)$$

It follows that coalescence of a simulation particle against field particles is a Poisson process and that the the rate of coalescence events,  $\chi_i(v)$  [1/s], for a simulation particle,  $v$ , against a particular field particle,  $y_i$ , is:

$$\chi_i(v) = \left( \frac{M}{NV_{cell}} \right) \frac{K(v,y_i)}{\rho_{liq} y_i} \quad (23)$$

The total coalescence rate against all field particles becomes:

$$\chi(v) = \sum_i \chi_i(v) = \left( \frac{M}{\rho_{liq} NV_{cell}} \right) \sum_i \frac{K(v,y_i)}{y_i} \quad (24)$$

This leads to the following scheme for coalescence events:

1. In a time step,  $\Delta t$ , select the number of coalescence events,  $n$ , randomly from a Poisson distribution with parameter  $\chi(v) \Delta t$ .
2. Pick  $n$  values,  $y_j$ ,  $j=1,2..n$ , randomly with probability  $P_i = \chi_i(v) / \chi(v)$  from the field particles (with replacement). Then update the simulation particle size as  $v := v + \sum_{j=1}^n y_j$

Note that more than one coalescence event during a time step should be a rare event. If not, the time step is too large and should be decreased.

## Handling breakup

There are a number of published breakup kernels in the literature (Liao and Lucas (2009)). Thus, select a breakup frequency model,  $\Gamma(v)$ . Select the number of breakages,  $n_{break}$  during a time step from a Poisson distribution with parameter  $\Gamma(v) \Delta t$ . Again, the time step should be sufficiently small that 0 and 1 events during the time step dominate.

For each breakup event we use Monte Carlo selection, and sample one daughter from the daughter distribution,  $\beta_m(v|v')$ , as explained in the section "Application of selection to breakup events" above. The cumulative daughter distribution is given by

$$F(v) = \int_0^v \beta_m(v|v') dv \quad (25)$$

The distribution can then be sampled by the inverse distribution method as  $v/v' = F^{-1}(\xi)$  where  $\xi$  is a uniform on [0 – 1] random number.

## VALIDATION OF THE METHODOLOGY

The methodology has been validated against analytical results for breakup and coalescence in Continuous Stirred Tank

Reactors (CSTR). A CSTR is similar to a single Finite Volume cell in the CFD code, and the methodology can be directly applied. For the validation we have used simple Matlab scripts.

### Case 1. CSTR with pure breakup

First, we demonstrate that the Monte Carlo selection procedure results in a correct daughter distribution. As a test case, we use 'Case 1' of Attarakih *et al.* (2004), for which there is an analytical solution.

Consider a Continuous Stirred Tank Reactor (CSTR). Assuming no spacial gradients, the population balance (1) can be integrated over the CSTR volume. Assuming no coalescence the population balance becomes

$$\begin{aligned} \frac{\partial m(v)}{\partial t} &= \frac{m_{feed}(v) - m(v)}{\tau} - \Gamma(v) m(v) \\ &+ \int_v^\infty \Gamma(v') \beta_m(v|v') m(v') dv' \end{aligned} \quad (26)$$

where  $m_{feed}$  is the feed distribution and  $\tau$  is the CSTR residence time.

The test case is:

$$\frac{m_{feed}(v)}{\rho_{liq}} = \frac{1}{v_0} \exp\left(-\frac{v}{v_0}\right) \quad (27)$$

$$\Gamma(v) = k_b \frac{v}{v_0} \quad (28)$$

$$\beta_m(v|v') = \frac{2v}{v'^2} \quad (29)$$

where  $v_0$  [ $m^3$ ] and  $k_b$  [1/s] are parameters.

Applying the described methodology, we arrive at the following algorithm. We select a fixed time step  $\Delta t$  that is sufficiently small compared to  $1/\Gamma$ .

1. **New simulation particle.** Select the size,  $v$ , of the simulation particle randomly from the feed distribution,  $m_{feed}$  (here: the exponential distribution with parameter  $v_0$ ).
2. **Outlet flow.** Particle can leave the CSTR during the time step  $\Delta t$ . This is a Poisson process. Thus, select a random number,  $n$ , from the Poisson distribution with parameter  $\Delta t / \tau$ . If  $n > 0$  the particle left the tank. Pick a new particle by restarting at step 1. Otherwise,  $n = 0$  and we continue with the next step.
3. **Particle breakage.** Select the number of breakages during the time step  $\Delta t$  from a Poisson distribution with parameter  $\Gamma \Delta t$ . The time step should be so small that two or more breakages during  $\Delta t$  happens rarely<sup>2</sup>. Zero and one events should dominate.
4. **Splitting into daughters.** By Monte Carlo splitting, select one daughter randomly from the  $\beta_m$ -distribution. In the present case we can select  $v = \sqrt{\xi} v'$  where  $\xi$  is a uniform on [0 – 1] random number<sup>3</sup>. Continue from step 2.

<sup>2</sup>In the present example we could select the time between events from an exponential distribution with parameter  $1/\Gamma$ , resulting in a variable time step  $\Delta t$ . However, in the CFD application this becomes impractical.

<sup>3</sup>The cumulative distribution of  $\beta_m$  is  $F(v) = \int_0^v \beta_m(v|v') dv = (v/v')^2$ . The inverse distribution method yields  $v/v' = F^{-1}(\xi)$ , or  $v = \sqrt{\xi} v'$ .

The analytical solution of Attarakih *et al.* (2004) at steady state can be written as

$$\frac{m(v)}{\rho_{liq}} = C v \left( \frac{1}{a} + \frac{2k_b \tau}{a^2} + \frac{2(k_b \tau)^3}{a^3} \right) \quad (30)$$

$$a = 1 + k_b \tau \frac{v}{v_0} \quad (31)$$

where  $C$  is a normalization constant.

Figure 4 shows a comparison between the cumulative mass distribution in our approach<sup>4</sup> and the analytical solution using  $N = 10\,000$  simulation particles,  $\tau = 100$  s,  $k_b = 1$  s<sup>-1</sup>,  $\Delta t = 1$  s and  $v_0 = 1$  mm<sup>3</sup>. As can be seen, the correspondence is excellent.

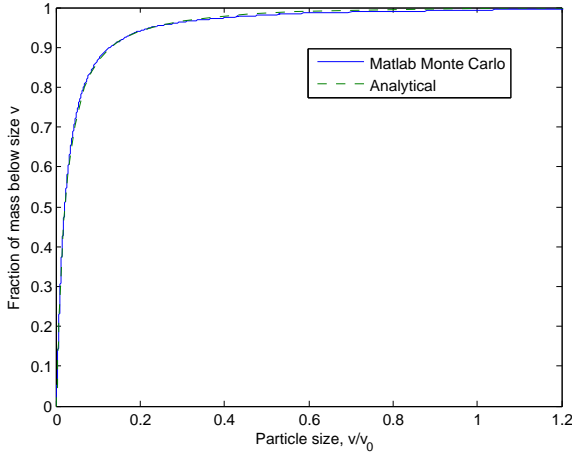


**Figure 4:** Case 1. Validation of daughter distribution from breakup.  $N = 10\,000$  simulation particles,  $\tau = 100$  s,  $k_b = 1$  s<sup>-1</sup>,  $\Delta t = 1$  s and  $v_0 = 1$  mm<sup>3</sup>.

## Case 2. CSTR with coalescence

We consider coalescence in a CSTR. Assuming no breakup and a constant breakup kernel,  $K(v, v') = K_0$ , the population balance becomes

$$\begin{aligned} \frac{\partial m(v)}{\partial t} = & \frac{m_{feed}(v) - m(v)}{\tau} \\ & + \int_0^v \frac{K_0}{\rho_{liq} v'} m(v') m(v-v') dv' \\ & - \int_0^\infty \frac{K_0}{\rho_{liq} v'} m(v') m(v) dv' \end{aligned} \quad (32)$$

where  $m_{feed}$  is the feed distribution and  $\tau$  is the CSTR residence time. The inlet mass distribution of the test case is

$$\frac{m_{feed}(v)}{\rho_{liq} N_0 v_0} = \frac{v}{v_0^2} \exp\left(-\frac{v}{v_0}\right) \quad (33)$$

where  $N_0$  and  $v_0$  are parameters.

An analytical solution to this problem is given in Nicmanis and Hounslow (1998) as

$$m(v) = \rho_{liq} N_0 \frac{v}{v_0} \frac{I_0\left(\frac{-tv}{v_0(1+2t)}\right) + I_1\left(\frac{-tv}{v_0(1+2t)}\right)}{\sqrt{1+2t} \exp\left[\frac{(1+t)v}{(1+2t)v_0}\right]} \quad (34)$$

<sup>4</sup>As all simulation particles represent the same amount of mass in our formulation, the plot is simply the accumulated mass fraction  $F = [1/N, 2/N, \dots, N/N]$  against a sorted vector of the simulation particles leaving the reactor,  $[v_1, v_2, \dots, v_N]$ .

where  $t = K_0 N_0 \tau$  and  $I_0, I_1$  are modified Bessel functions. Nicmanis and Hounslow (1998) also explain how to avoid overflow/underflow when evaluating this expression by using the asymptotic expression

$$m(v) = \rho_{liq} v \frac{\exp\left(\frac{-v}{2v_0 t}\right)}{\sqrt{\pi}(2t)^2 \left[\frac{v}{2v_0 t}\right]^{3/2}} \quad (35)$$

which is used when

$$\frac{-tv}{v_0(1+2t)} > 700 \quad (36)$$

We apply the algorithm given in sections through using  $N = 50\,000$  simulation particles,  $\tau = 200$  s,  $K_0 = 1$  mm<sup>3</sup>/s,  $N_0 = 1$  mm<sup>-3</sup>,  $v_0 = 1$  mm<sup>3</sup>,  $\Delta t = 2$  s,  $\beta = 0.01$ ,  $N_{field} = 100$  field particles,  $\lambda = 0.01 N_{field} / \tau = 0.005$ .

The resulting cumulative mass distribution is shown in Figure 5. The match between our scheme and the analytical result is excellent.

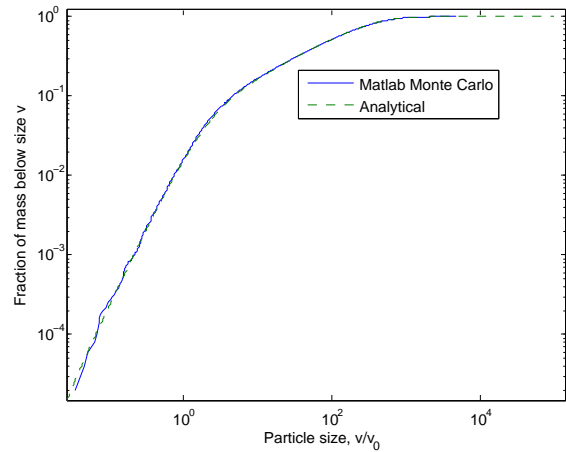


**Figure 5:** Case 2. Validation of coalescence using  $N = 50\,000$  simulation particles,  $\tau = 200$  s,  $K_0 = 1$  mm<sup>3</sup>/s,  $N_0 = 1$  mm<sup>-3</sup>,  $v_0 = 1$  mm<sup>3</sup>,  $\Delta t = 2$  s,  $\beta = 0.01$ ,  $N_{field} = 100$  field particles,  $\lambda = 0.01 N_{field} / \tau = 0.005$ .

## VALIDATION OF THE FLUENT IMPLEMENTATION

In order to validate the FLUENT implementation, we have simulated a simple plug flow reactor, as shown in Figure 6. Since this is a very simple problem it can be compared against the Matlab scripts that was validated in Case 1 and 2.

We emphasize that our implementation inherits all the functionality of the FLUENT DPM model. I.e. it works for unstructured 3D meshes, with momentum coupling between the particles and the continuous fluid, various boundary conditions etc. See the FLUENT theory guide (Ansys Inc., Nov. 2010) for details about functionality.

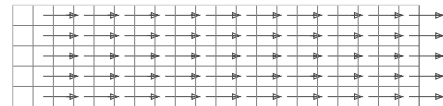


**Figure 6:** Case 3. Simple FLUENT mesh for plug flow test

## Validation of breakup implementation

The plug flow parameters used to validate the breakup implementation in FLUENT are identical to Case 1 above except for the plug flow aspect. The residence time in the reactor is 100 s as before.

As a comparison, we use the algorithm in section except that we replace the residence time in step 2 with the fixed value  $\tau$ . We reuse the Matlab script that was used for the Case 1 validation.

Figure 7 shows a comparison between the outlet size distribution by the FLUENT model and the corresponding Matlab result. The correspondence is excellent.

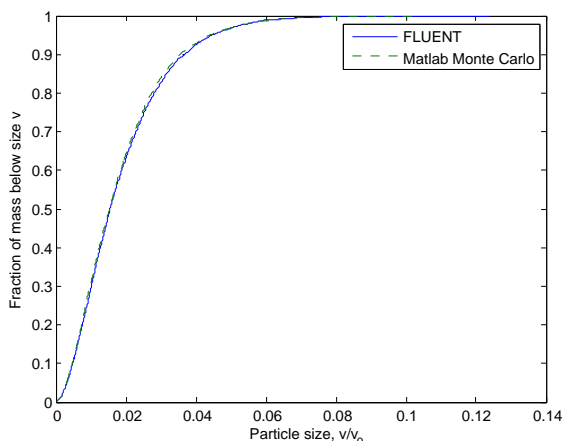


**Figure 7:** Case 3. Validation of daughter distribution from breakup using FLUENT.  $N = 10\,000$  simulation particles,  $\tau = 100$  s,  $k_b = 1\text{ s}^{-1}$  and  $v_0 = 1\text{ mm}^3$ .

## Validation of coalescence implementation

The plug flow parameters used to validate the coalescence implementation in FLUENT are identical to Case 2 above except for the plug flow aspect. The residence time in the reactor is 200 s as before. We use 10 field particles per cell; parameters  $\beta = 0.001$  and  $\lambda = 0.01$  in FLUENT.

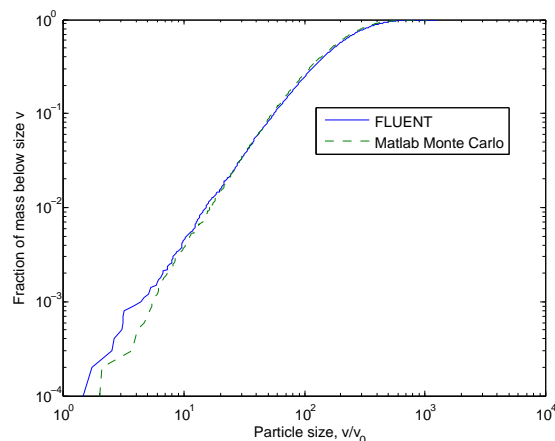
As a comparison we couple 20 CSTR's in series. We reuse the Matlab script for coalescence in a CSTR that was validated in Case 2.

Figure 8 shows a comparison between the outlet size distribution by the FLUENT model and the corresponding Matlab result. The correspondence is quite good. Note that there is inevitably a discrepancy at the tails of the distribution. Since we use 10000 particles, there are only 100 particles below an accumulated mass fraction of  $10^{-2}$ , and only 10 particles below  $10^{-3}$ .

## DISCUSSION AND CONCLUSION

One of the nice properties of the scheme presented in this paper is that there is global conservation of mass and momentum. A simulation particle has the same mass flow along the particle track even when there is breakup and coalescence. Thus, droplet mass will never appear or disappear.

The present paper focus on the general methodology, and not on actual kernels for coalescence and breakup. This is a subject of a subsequent paper. In turbulent flows one inevitably



**Figure 8:** Case 4. Validation of FLUENT daughter distribution from coalescence.  $N = 10\,000$  simulation particles,  $\tau = 200$  s,  $K_0 = 1\text{ mm}^3/\text{s}$ ,  $\beta = 0.001$ ,  $N_{field} = 10$  field particles per cell,  $\lambda = 0.01$  and  $v_0 = 1\text{ mm}^3$ .

has to make closure models when modelling coalescence and breakup. One of the purposes of our FLUENT model is to enable us to compare the predictions of coalescence and breakup kernels against experimental data.

In conclusion, the Monte Carlo, Single Particle method developed in this article can predict the solution of population balance equations. It is applicable to population balances in general, and in particular to droplet breakup and coalescence in gas-liquid flow. It has been shown how methods developed for Neutron transport, such as Monte Carlo splitting and selection, is directly applicable to population balances in Chemical Engineering applications.

The method has been implemented on top of the existing Discrete Particle Model (DPM) in FLUENT. Thus we have added population balance functionality to the DPM model without limiting the functionality of the DPM model.

The method has been validated against analytical solutions for breakup and coalescence.

## REFERENCES

- Anslys Inc. (Nov. 2010). *ANSYS FLUENT Theory Guide, Release 13.0*.
- ATTARAKIH, M., BART, H. and FAQIR, N. (2004). "Numerical solution of the spatially distributed population balance equation describing the hydrodynamics of interacting liquid-liquid dispersions". *Chemical Engineering Science*, **59**, 2567–2592.
- ATTARAKIH, M., DRUMM, C. and BART, H. (2009). "Solution of the population balance equation using the sectional quadrature method of moments (sqmom)". *Chemical Engineering Science*, **64**, 742–752.
- DORAO, C. and JAKOBSEN, H. (2005). "Application of the least square method to population balance problems". *Computers and Chemical Engineering*, **30**, 535–547.
- HAVILAND, J. and LAVIN, M. (1962). "Application of the monte carlo method to heat transfer in a rarified gas". *Physics of Fluids*, **11**, 1399–1405.
- JIANG, B. (1998). *The Least-Square Finite Element Method: Theory and Applications in Computational Fluid Dynamics and Electromagnetics*. Springer, Berlin.

LUX, I. and KOBLINGER, L. (1991). *Monte Carlo particle transport methods : Neutron and photon calculations*. Boca Raton : CRC Press, Cambridge.

MCGRAW, R. (1997). "Description of aerosol dynamics by the quadrature method of moments". *Aerosol Science and Technology*, **27**, 255–265.

MORUD, J. (2011). "Implementation of the sectional quadrature method of moments in fluent". *8th International Conference on CFD in Oil and Gas, Metallurgical and Process Industries SINTEF/NTNU, Trondheim Norway*.

NICMANIS, M. and HOUNSLOW, M.J. (1998). "Finite-element methods for steady-state population balance equations". *AIChE Journal*, **44(10)**, 2258–2272. URL <http://dx.doi.org/10.1002/aic.690441015>.

RAMKRISHNA, D. (2000). *Population balance-Theory and Applications to Particulate Processes in Engineering*. Academic Press, San Diego.

VIKHANSKY, A. and KRAFT, M. (2005). "Single-particle method for stochastic simulation of coagulation processes". *Chemical Engineering Science*, **60**, 963–967.